

  UNIVERSITAT POLITÈCNICA
DE CATALUNYA
BARCELONATECH
Campus d'Excel·lència Internacional

Doctoral training seminars: track microelectronics

Emergent enabling technologies for wireless data, energy processing and communications

PhD students: Ignacio Llatser¹, Sergi Abadal¹, Mario Iannazzo¹, Albert Mestres¹, Julià Delós¹, Raul Gomez Cid-Fuentes¹, Elisenda Bou¹
 Faculties: Alberto Cabellos¹, Josep Jornet^{1,2}, Mario Nemirovsky³, Max Lemme⁴, Josep Solé-Pareta¹, Heekwan Lee⁵, Ian F. Akyildiz^{1,2}
 Peter Fisher⁶, Tomas Palacios⁶, Kaushik Chowdhury⁶

¹ UPC BarcelonaTech and Nanonetworking Center (N3Cat-UPC)
² GeorgiaTech, Atlanta, US
³ BSC Barcelona Supercomputing Center
⁴ Royal Institute of Technology, KTH Stockholm, Sweden,
⁵ Samsung Advanced Institute of Technology, Seoul, South Korea
⁶ Massachusetts Institute of Technology, MIT, Cambridge, US

Graphene-enabled wireless comms: Team and projects

● “Graphene-enabled Wireless Communications” funded by the **Samsung Advanced Institute of Technology** (Seoul, Korea) under the GRO gift program

● “Graphene antennas for Wireless Networks-on-chip” by **Intel research**

● EU FET flagship project “Graphene”

● EU FET flagship project “Guardian Angels”

● EU FET flagship project “Human Brain project”

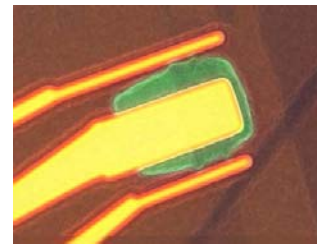
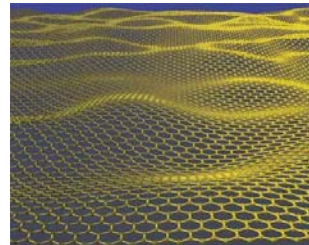




 Dr. Albert Cabellos (AC)  UNIVERSITAT POLITÈCNICA DE CATALUNYA BARCELONATECH	 Prof. Ian Akyildiz (UPC Hon.) 
 Ignacio Llatser  UNIVERSITAT POLITÈCNICA DE CATALUNYA BARCELONATECH	 Dr. Mario Nemirovski  BSC Barcelona Supercomputing Center 
 Josep Miquel Jornet (UPC, MIT) 	 Prof. Max Lemme 
 Prof. Eduard Alarcón (EE)  UNIVERSITAT POLITÈCNICA DE CATALUNYA BARCELONATECH	 Prof. Tomas Palacios  MIT Massachusetts Institute of Technology

Grafè**Grafè**

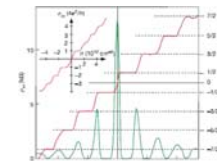
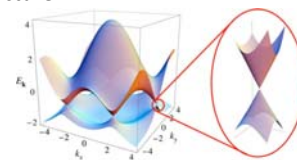
- Capa de carboni monoatòmic (d'un sol àtom de gruix)
- Xarxa cristal·lina en forma de niu d'abella
- Descobert per A. K. Geim i K. S. Novoselov el 2004
- Aquest descobriment els va valer el premi Nobel de física



3

Grafè**Quines són les propietats extraordinàries del grafè que han atret l'atenció d'investigadors al voltant del món?**

- Material més fi i lleuger observat a la natura (0.3 nanometers)
- Més dur que el diamant
- 300 cops més resistent que l'acer (Young modulus 1 TPa (Steel ~ 0.2 TPa))
- Condueix l'electricitat molt millor que el coure
- Transparent (97.7% optical transparency)
- Flexible: pot prendre qualsevol forma
- One-atom-thick impermeable membrane
- Gapless energy band structure



4

Grafè

N3Cat

- Nano-electrònica
 - Transistors i circuits integrats ultra-ràpids
 - Super-condensadors (bateries)
 - Efecte piezoelectric a la nano-escala
- Nano-òptica
 - Nano-làsers
 - Moduladors òptics
- Tecnologies de la informació i les comunicacions
 - Comunicacions de rang ultra-curt basades en antenes de grafè

Mid-term: Graphene-based Wireless Network-on-Chip for Multi-Core processors

Long-term: Wireless Nano-Sensor Networks (WNSN)

I. F. Akyildiz, J. M. Jornet, "The Internet of Nano-Things", IEEE Wireless Communications, 2010.
S. Abadal, A. Cabellos-Aparicio, J. A. Lázaro, E. Alarcón, J. Soté-Pérez, "Graphene-enabled hybrid architectures for multiprocessors: bridging nanophotonics and nanoscale wireless communication," in Proc. of the International Conference in Transparent Optical Networks (ICTON), 2012.

5

Downscaling a traditional antenna

N3Cat

First resonant frequency [THz]

Antenna length [μm]

$f_{0\text{Au}} = \Theta(1/L_{\text{eff}})$

- Downscaling a traditional antenna to a few um is not possible
- Radiation frequency in the Optical Regime
- Downscalability factor: $\Theta(1/L_{\text{eff}})$

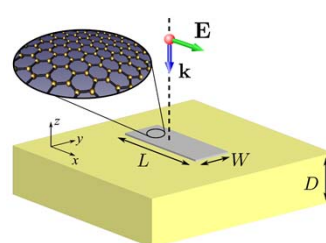
I. Llatser, C. Kremers, A. Cabellos-Aparicio, E. Alarcón and D. N. Chigrin, "Comparison of the Resonant Frequency in Graphene and Metallic Nano-antennas", in AIP Conference Proceedings, 2012

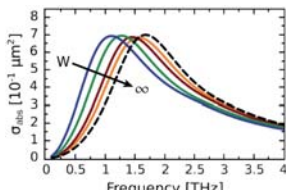
6

Graphene antennas at THz band

N3Cat

- Explore antennas that resonate
 - much lower frequency than optical regime
 - High end of the EM RF band
- Graphene-based plasmonic nano-antennas (graphennas)
 - Size in the μm range
 - Predicted to radiate in the THz band



$$\sigma(\omega) = \frac{2e^2}{\pi\hbar} \frac{k_B T}{\hbar} \ln \left[2\cosh \left[\frac{\mu_c}{2k_B T} \right] \right] \frac{i}{\omega + i\tau^{-1}}$$


Frequency (Hz) 10^0 10^3 10^6 10^9 10^{12} 10^{15} 10^{18} 10^{21}

Electronics
Microwaves
MF, HF, VHF, UHF, SHF, EHFs
THz
Photonics
Visible
X-ray
 γ -ray

kilo mega giga tera peta exa zetta

● EU FET flagship project "Graphene"

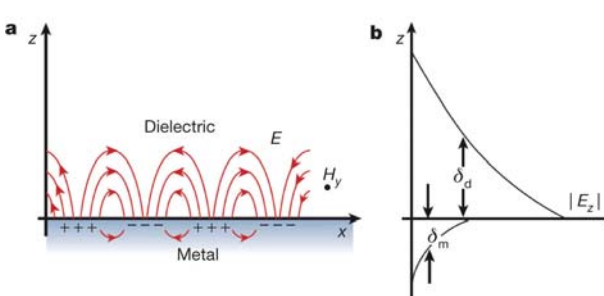
GRAPHENE FLAGSHIP

7

Analysis of graphene RF plasmonic antennas

N3Cat

- In order to understand the behavior of graphennas, we need to study the propagation of **Surface Plasmon Polariton (SPP)** waves in graphene
 - EM waves guided along a metal-dielectric interface which are generated by an incident high-frequency radiation



O. Benson, "Assembly of hybrid photonic architectures from nanophotonic constituents", *Nature*, 2011.

8

Analysis of graphene RF plasmonic antennas



- In order to calculate the resonant frequency of graphennas, we consider their **dispersion relation**

- Relates the wavenumber with the frequency of SPP waves propagating in a graphene layer

$$\frac{1}{\sqrt{k_{\text{SPP}}^2 - \frac{\omega^2}{c^2}}} + \frac{\epsilon}{\sqrt{k_{\text{SPP}}^2 - \epsilon \frac{\omega^2}{c^2}}} = -i \frac{\sigma(\omega)}{\omega \epsilon_0}$$

ϵ : dielectric constant of the substrate
 ϵ_0 : dielectric constant of vacuum
 β : wavenumber
 ω : angular frequency
 c : speed of light
 $\sigma(\omega)$: conductivity of graphene

$$n_{\text{eff}}(\omega) = \sqrt{1 - 4 \frac{\mu_0}{\epsilon_0} \frac{1}{\sigma(\omega)^2}}$$

The graphene conductivity will determine the properties of SPP in graphene

Marinko Jablan, Hrvoje Buljan and Marin Soljačić, "Plasmonics in graphene at infrared frequencies" PHYSICAL REVIEW B 80, 245435 2009 (MIT)

Analysis of graphene RF plasmonic antennas



- The frequency-dependent **electrical conductivity** of a graphene monolayer is obtained using the random-phase approximation

$$\sigma(\omega) = \frac{2e^2}{\pi h} \frac{k_B T}{\hbar} \ln \left[2 \cosh \left[\frac{\mu_c}{2k_B T} \right] \right] \frac{i}{\omega + i\tau^{-1}}$$

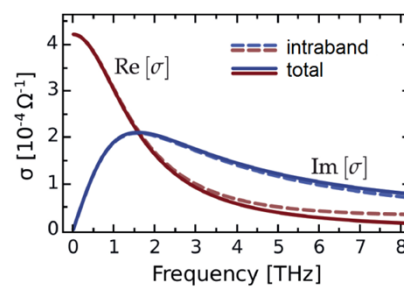
intraband contribution

$$\sigma_i(\omega) = \frac{e^2}{4h} \left(H\left(\frac{\omega}{2}\right) + i \frac{4\omega}{\pi} \int_0^\infty d\epsilon \frac{H(\epsilon) - H(\omega/2)}{\omega^2 - 4\epsilon^2} \right)$$

$$H(\epsilon) = \frac{\sinh(\hbar\epsilon/k_B T)}{\cosh(\mu_c/k_B T) + \cosh(\hbar\epsilon/k_B T)}$$

$\sigma(\omega)$: conductivity of graphene
 ω : angular frequency
 e : electron charge
 \hbar : reduced Planck's constant
 k_B : Boltzmann's constant
 T : temperature
 μ_c : chemical potential
 τ : relaxation time

interband contribution



10

Analysis of graphene RF plasmonic antennas

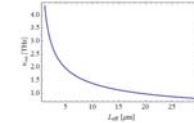


- The graphene patch acts as a Fabry-Perot resonator for SPP waves with the resonance condition

$$(1) \quad L = L' + 2\delta L = m \frac{\lambda_{\text{SPP}}}{2} = m \frac{\pi}{k_{\text{SPP}}} \quad \begin{array}{l} L: \text{effective antenna length} \\ k_{\text{SPP}}: \text{SPP wavenumber} \\ \lambda_{\text{SPP}}: \text{SPP wavelength} \\ m: \text{resonance order} \end{array}$$

- By combining the resonance condition (1) with the dispersion relation in graphene (2), we can obtain the resonant frequency of graphennas as a function of their length

$$(2) \quad \frac{1}{\sqrt{k_{\text{SPP}}^2 - \frac{\omega^2}{c^2}}} + \frac{\epsilon}{\sqrt{k_{\text{SPP}}^2 - \epsilon \frac{\omega^2}{c^2}}} = -i \frac{\sigma(\omega)}{\omega \epsilon_0}$$



11

Analysis of graphene RF plasmonic antennas



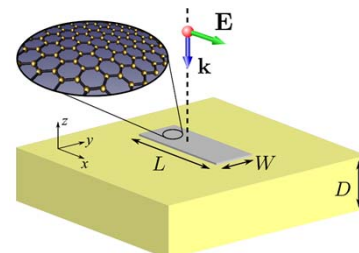
- The resonant frequency of graphennas can also be obtained by means of FEM electromagnetic simulations
 - Solve Maxwell's equations numerically with the appropriate boundary conditions
- An incident plane wave normally incident to the antenna is considered

$$\oint \mathbf{E} \cdot d\mathbf{A} = \frac{Q}{\epsilon_0}$$

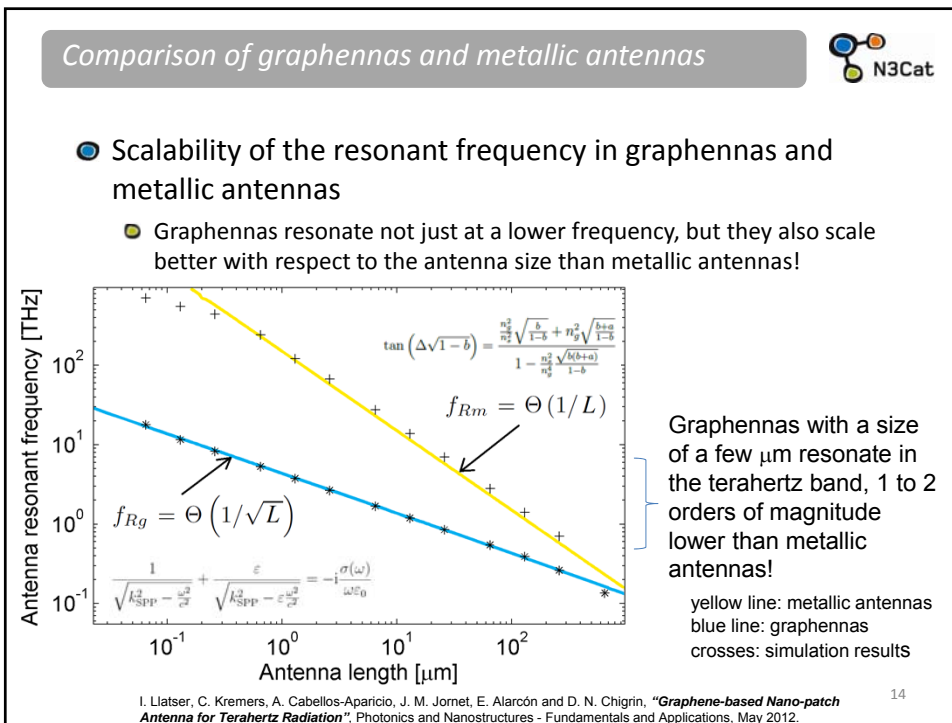
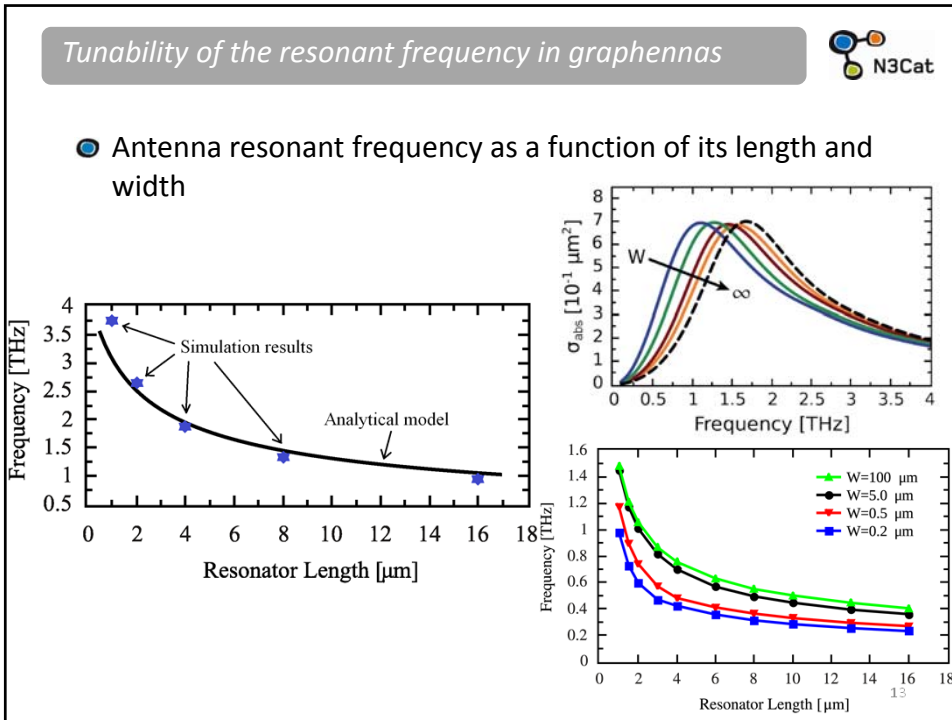
$$\oint \mathbf{B} \cdot d\mathbf{A} = 0$$

$$\oint \mathbf{E} \cdot d\mathbf{s} = -\frac{d\Phi_m}{dt}$$

$$\oint \mathbf{B} \cdot d\mathbf{s} = \mu_0 I + \epsilon_0 \mu_0 \frac{d\Phi_e}{dt}$$



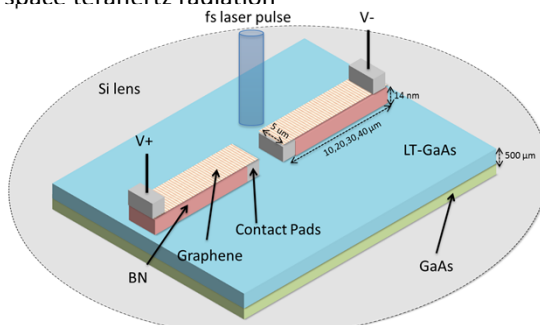
12



Photoconductive-fed graphennas



- A practical technique to feed graphennas is by means of photoconductive sources
 - Laser radiation excites photocarriers in the biased semiconductor and generates terahertz pulses
 - The excitation of SPP waves in the dipole graphenna produces a free-space terahertz radiation

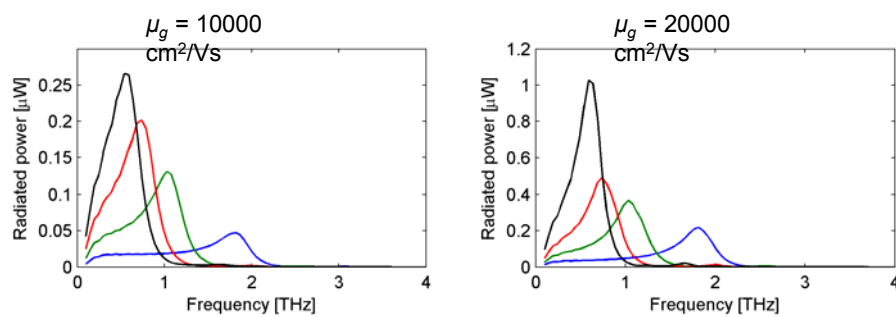
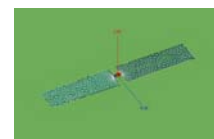


A. Cabellos-Aparicio, I. Llatser, E. Alarcón, A. Hsu and T. Palacios, “**Use of THz Photoconductive Sources to Characterize Graphene RF Plasmonic Antennas**”, IEEE Transactions on Nanotechnology (UPC / MIT –ECE-)

Photoconductive-fed graphennas



- Power radiated by the photoconductive graphenna, for different antenna lengths
 - Frequency content in the terahertz band
 - Increases with the electron mobility in graphene



16

Operational range of graphene antennas

N3Cat

- How graphene antennas downscalability advantage compares to metallic antennas?

A. Cabellos, I. Llatser, E. Alarcón, A. Hsu, and T. Palacios, Max Lemme, Mikael Östling
B. (UPC / MIT / KTH / Ericsson)

17

Application 1: wireless multicore processors

N3Cat

- Computer performance improvement is no longer achievable by simply increasing the operation frequency
 - Heat
 - Power consumption
 - Current leakage

→ **Emergence of manycore processors**

- The performance bottleneck of multicore processors has shifted from clock frequency to inter-core communication capabilities.
 - Need of new scalable communication techniques

→ **Comms Network-on-Chip (NoC)**

18

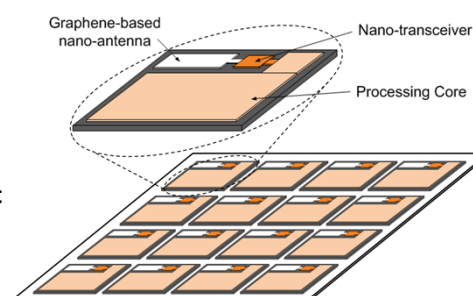
Graphene-enabled Hybrid Optical/Wireless NoC (II)



Graphene microantennas for wireless Network-on-Chip architectures

WHY WIRELESS for NOC?

- Multi-user shared RF medium
- Latency
- Reconfigurability
- Inherent broadcast and multicast
- 3D FFT supercomputers and
- Big Data (Google)





PhD Candidate Sergi Abadal "Intel Doctoral Student Award"
"Graphene-enabled Wireless Communications for Manycore Architectures"



● EU FET flagship project "Human Brain project"

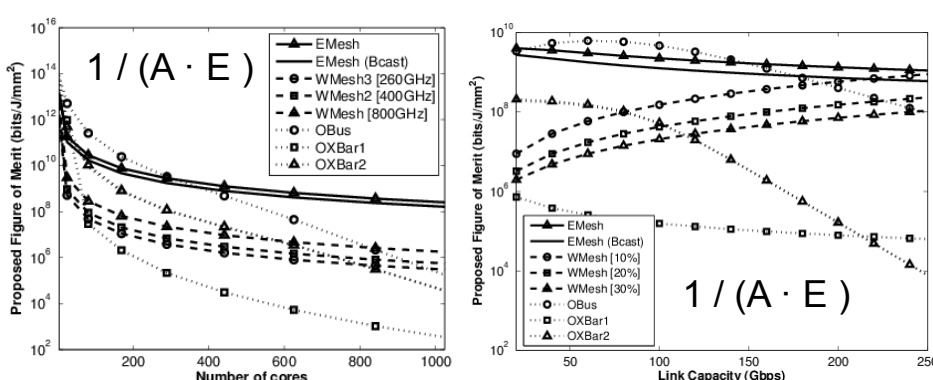
19

GWNoC: Feasibility Study



● Implementation-Communications

● How do area (A) and bit energy (E) scale?



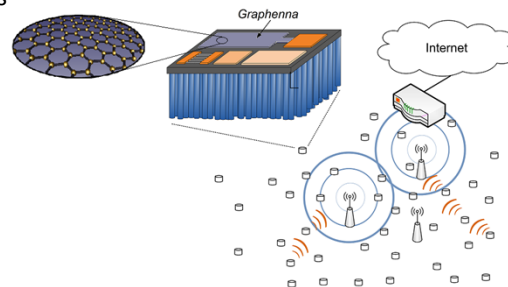
S. Abadal, M. Iannazzo, M. Nemirovsky, A. Cabellos-Aparicio, H. Lee, E. Alarcón, **"On the Area and Energy Scalability of Wireless Network-on-Chip: A Model-based Benchmarked Design Space Exploration"**, submitted for publication on IEEE Transactions on Networking, Oct. 2013, revision in process.

Aplicació 2: xarxes de nano-sensors sense fils



● Nano-sensor

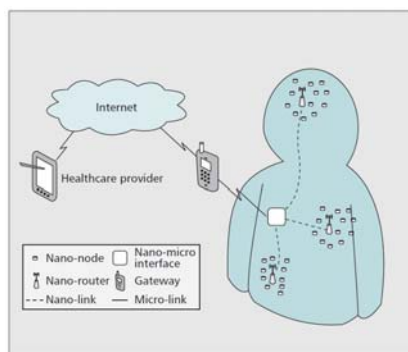
- Nanodispositius d'una dimensió de uns quants (pocs) micròmetres
- Capacitat de mesurar, processar i emmagatzemar informació
- I de recol·lectar l'energia que necessita per sensar i processar (*energy harvesting*), per exemple amb nanofils de zinc
- Equipats amb antenes de grafè per comunicar-se (via ràdio) amb d'altres nano-sensors



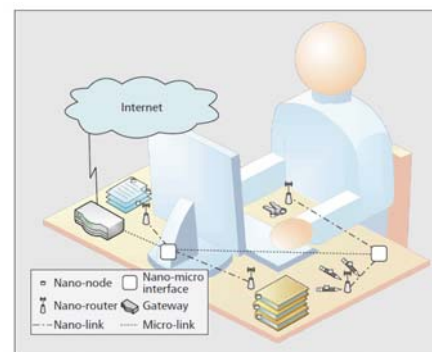
Aplicació 2: xarxes de nano-sensors sense fils



● Algunes aplicacions de les xarxes de nano-sensors:

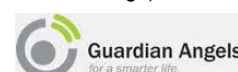


Sistema de detecció de malalties i administració cooperativa de medicaments
(Intrabody networks)



Internet de les nano-cooses
(Internet of nano-things)

● EU FET flagship project “Guardian Angels”

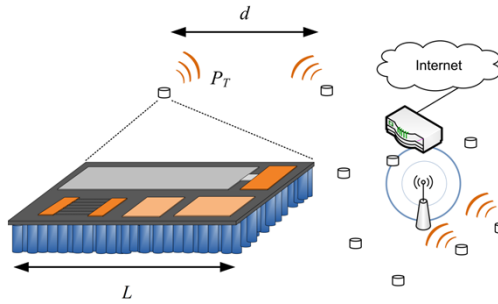


22

Channel capacity in GWC



- The scalability of the channel capacity in GWC is studied as a function of three scale parameters
 - Antenna length L
 - Transmission distance d
 - Transmitted power P_T
- The results using graphennas and metallic antennas are compared



23

Channel capacity in GWC



- The channel capacity is obtained with the Shannon-Hartley theorem, integrated over the whole terahertz band

$$C = \max_{S(f): \int_B S(f) df \leq P_T} \int_B \log_2 \left(1 + \frac{S(f)}{A(f)N(f)} \right) df$$

Transmitted power spectral density

$$S(f) = \begin{cases} P_T/B & \text{if } 0 < f < B, \\ 0 & \text{otherwise.} \end{cases}$$

Channel attenuation

$$A = A_{\text{spread}} A_{\text{abs}}$$

$$A_{\text{spread}} = \left(\frac{4\pi f d}{c} \right)^2$$

Noise power spectral density

$$N(f, d) = k_B(T_{\text{sys}} + T_{\text{mol}}(f, d))$$

$$A_{\text{abs}} = \frac{1}{\tau_m} = e^{k(f)d}$$

$$T_{\text{mol}}(f, d) = T_0(1 - e^{-k(f)d})$$

$$T_{\text{sys}} = T_0 = 293 \text{ K}$$

Bandwidth

$$B_m = \frac{k_1}{L} \quad B_g = \frac{k_2}{\sqrt{L}}$$

24

Channel capacity in GWC



Expression of the channel capacity in GWC

- The factor P_T/d^2 will have a key role

$$\begin{aligned}
 C(B, d, P_T) &= \int_0^B \log_2 \left(1 + \frac{P_T/B}{\left(\frac{4\pi f d}{c}\right)^2 N_0} \right) df \\
 &= \frac{B}{\log 2} \log \left(1 + \frac{c^2 P_T}{(4\pi d)^2 B^3 N_0} \right) + \frac{c\sqrt{P_T}}{2\log(2)\pi d\sqrt{N_0 B}} \arctan \frac{4\pi d B^{3/2} \sqrt{N_0}}{c\sqrt{P_T}} \\
 C_m(L, d, P_T) &= \frac{k_1}{\log(2)L} \log \left(1 + \frac{c^2 L^3 P_T / d^2}{(4\pi)^2 N_0 k_1^3} \right) + \frac{c\sqrt{L P_T / d^2}}{2\log(2)\pi\sqrt{N_0 k_1}} \arctan \frac{4\pi\sqrt{N_0 k_1^3}}{c\sqrt{L^3 P_T / d^2}} \\
 C_g(L, d, P_T) &= \frac{k_2}{\log(2)\sqrt{L}} \log \left(1 + \frac{c^2 L^{3/2} P_T / d^2}{(4\pi)^2 N_0 k_2^3} \right) + \frac{c\sqrt[4]{L} \sqrt{P_T / d^2}}{2\log(2)\pi\sqrt{N_0 k_2}} \arctan \frac{4\pi\sqrt{N_0 k_2^3}}{c L^{3/4} \sqrt{P_T / d^2}}
 \end{aligned}$$

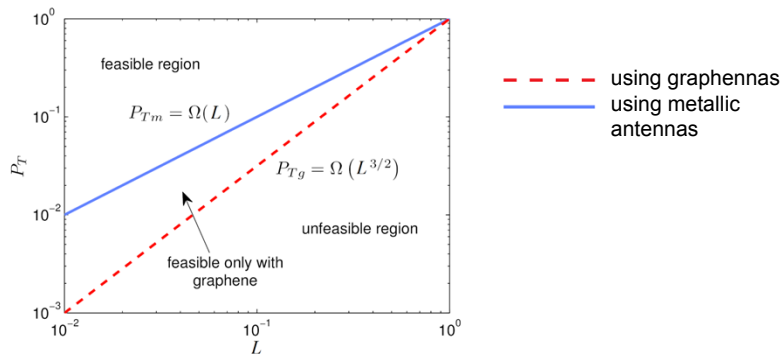
25

Channel capacity in GWC

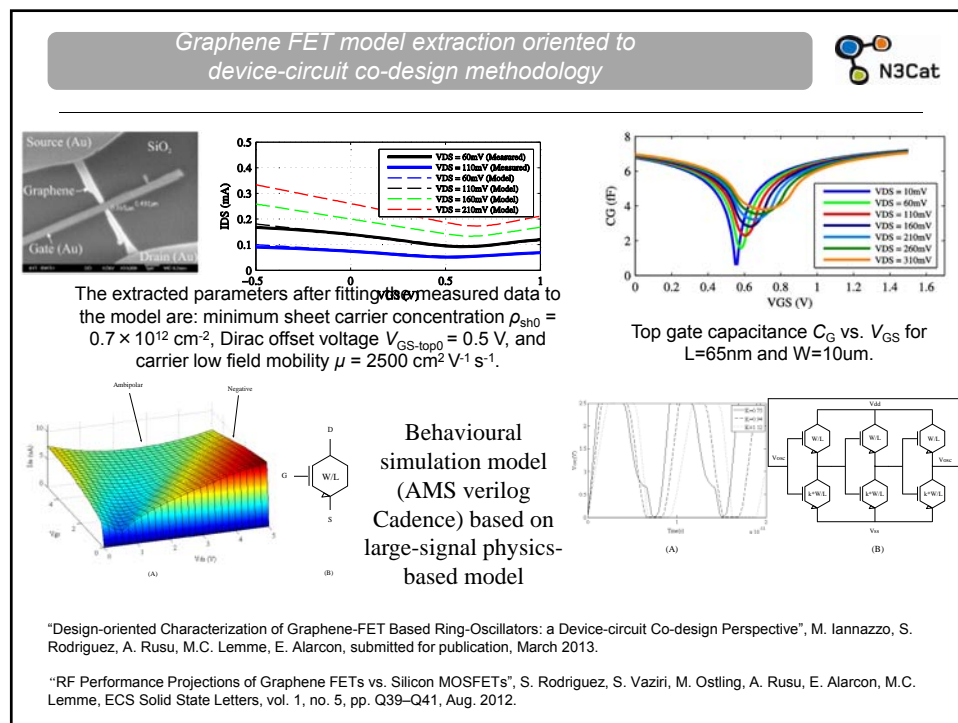
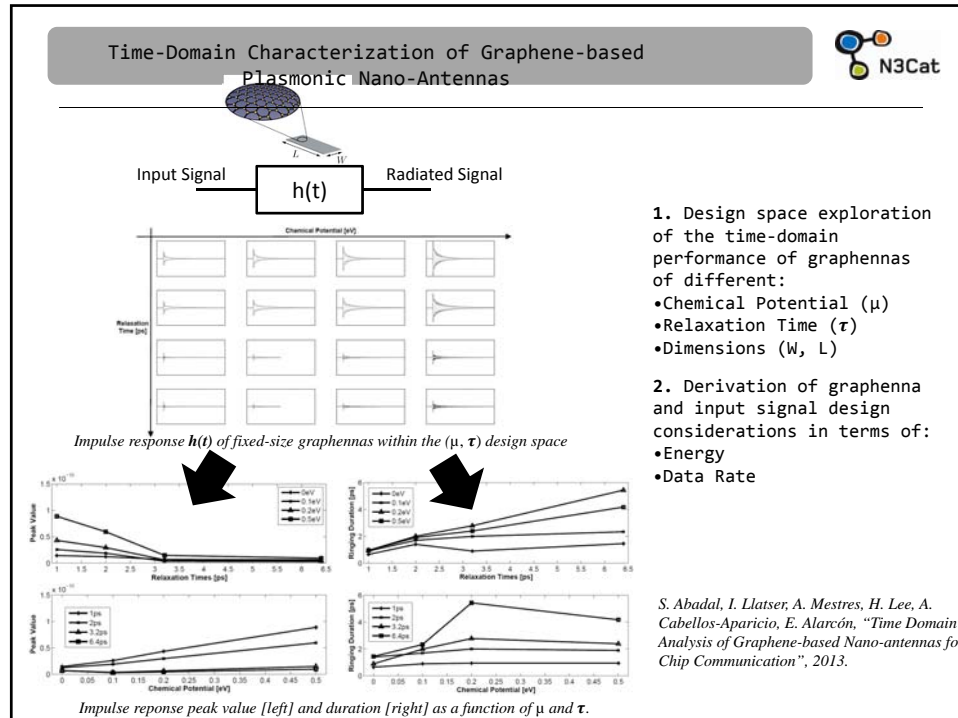


Scalability of the transmitted power in GWC with respect to the antenna length

- Additional feasibility condition: the network shrinks proportionally
 - Transmission distance scales proportionally to the antenna length ($\alpha=1$)
- Graphennas require less power than metallic antennas as their size is reduced to the nanoscale



26



On-chip energy Harvesting: Team and projects

Project: Energy Harvesting

CONSOLIDER-INGENIO 2010 (Spanish Ministry of Science and Technology), "Advanced Wide Band Gap Semiconductor Devices for Rational Use of Energy (RUE)", Principal Investigator: José Millán (CNM-CSIC, Bellaterra, Barcelona, Spain), Program period: Jan 2010 – Jan 2014, Investigators: 50 (CNM, UPM, UPC, UOvi, UZ, UPV, URV), Funding: 3MEuros

MCYT (Spanish Ministry of Science and Technology) (TEC2007-67988-C02-01) [coordinated project], "On-chip wideband adaptive energy management of RF power amplifiers: towards efficient next-generation mobile communications RF transmitters", PI: E. Alarcon (UPC) Program period: Jan 2008 – Dec 2010. Investigators: 12 (UPC, Universidad Pública de Navarra, Universidad Rovira i Virgili, Tarragona), Total: Euro 219K



Raul Gomez, PhD candidate

UNIVERSITAT POLITÈCNICA
DE CATALUNYA
BARCELONATECH



Prof. Eduard Alarcón (EE)

UNIVERSITAT POLITÈCNICA
DE CATALUNYA
BARCELONATECH



Prof. Kaushik Chowdhury
(Northeastern Univ Boston)

N3Cat

Device-design-oriented translayer model for tracking RF TX: system-to-device

WLAN stringent specs (BW 50 MHz)

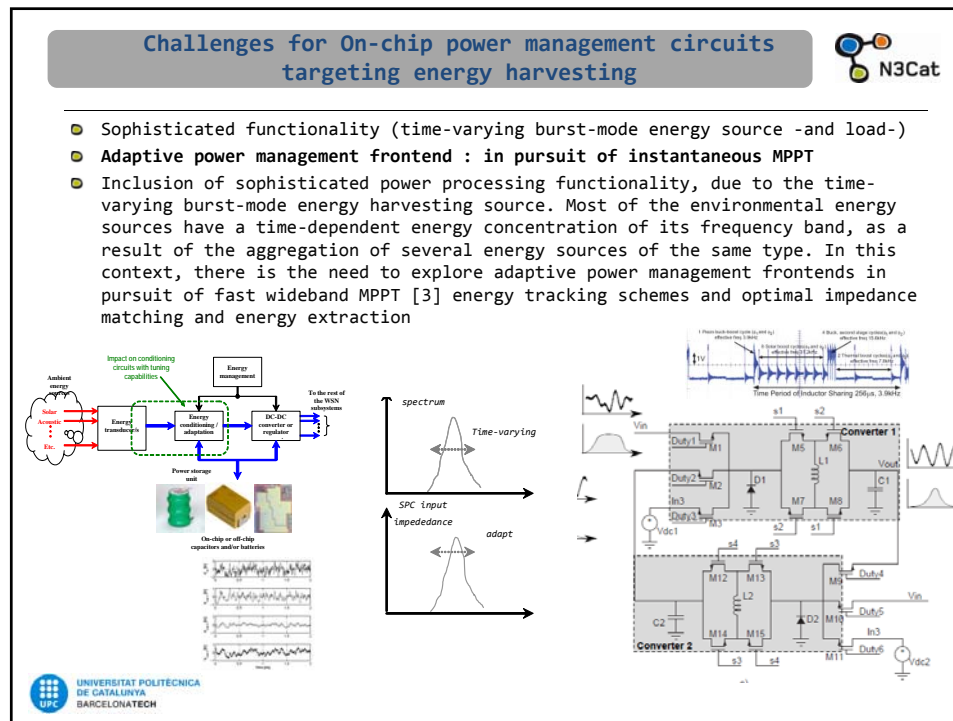
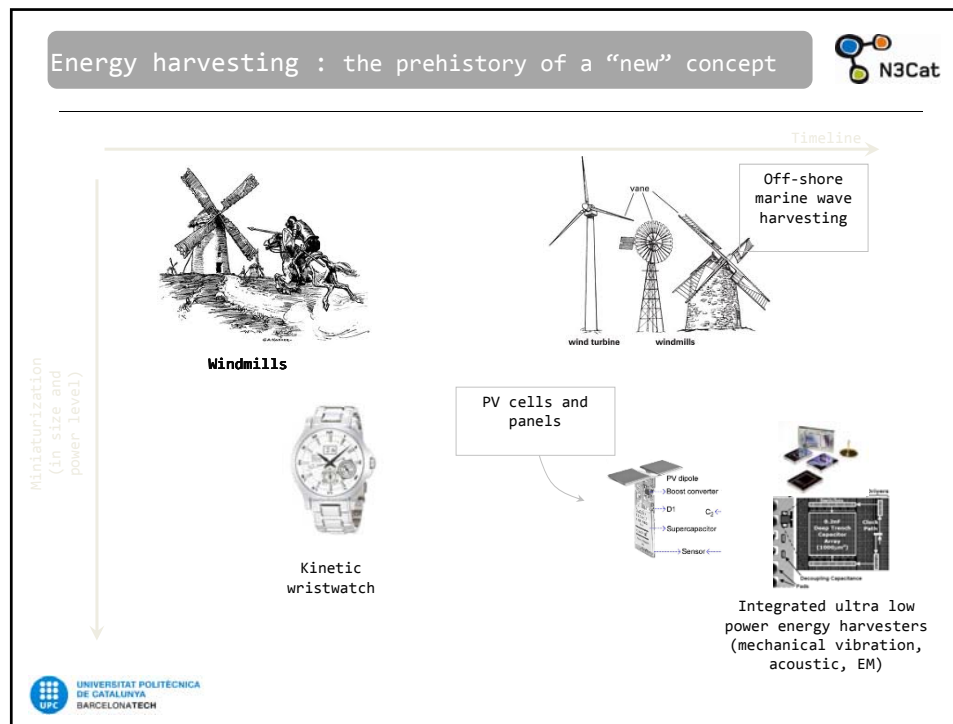
- Even with best topology (linear assisted multilevel) and control/modulation (nonlinear time optimal / asyn SD) efficiency is low in the available application/system-constrained design space
- Take behavioural model down to device level to derive guidelines and FOMs for next-generation (GaN) devices in terms of R_{on} and Q_s

Figure 6: WLAN TX signal spectra for the complete (f_s, f_o) design space

16-QAM scatter plots for different relevant configurations within the (f_s, f_o) design space

16-QAM EVMrms for configurations that fulfil (solid surface) or not (mesh surface) mode 5 EVM standard requirements.

J. Marchán "Device-design-oriented translayer model for Circuit/system design space characterization of EER-based transmitter for 802.11a WLAN Standard", IEEE International Symposium on Circuits and Systems, 2012, ISCAS 2010



Graphene-based vibration harvester

N3Cat

Frequency matching through nonlinear chaotic oscillation of graphene membrane mechanical harvester

Uncompressed or weakly compressed graphene membrane

$$\ddot{x} = -\frac{b}{m}\dot{x} - \frac{1}{m}\frac{\partial V}{\partial x} + \frac{\sigma^2}{m}\eta(t)$$

Figure 3. Dynamics of the graphene membrane under a stochastic external excitation $\sigma^2 = 1 \text{ pN}$ (red), $\sigma^2 = 50.5 \text{ pN}$ (green) and $\sigma^2 = 100 \text{ pN}$ (black). (a) Time series, (b) Trajectories in the phase plane (x, v). Equilibrium points of the free system are also plotted. (c) Probability density function (in dB) of the displacement x and (d) Smoothed FFT spectrum of the displacement x and noise $\sigma^2\eta(t)$. Note that the spectrum is spread to low frequency regions when the noise intensity is sufficiently large so that the potential barrier can be crossed.

"Nonlinear Dynamics in a Nanostructured Graphene Device for Energy Harvesting Applications", E. Alarcon et al., IEEE ISCAS 2013 Beijing, special session

UPC UNIVERSITAT POLITÈCNICA DE CATALUNYA BARCELONATECH

Ambient Energy model with dynamics separation and spatiotemporal correlation

N3Cat

- Spatio-Temporal Correlation of the Energy Field
- The Energy Path
- We discretize the state equation:
- Where:

$P_H(\mathbf{r}, t)$: Energy Field

n Sensor Nodes

$P_H(t) = P_S(t)p(t) [\text{W}]$

Communications

C_B : Energy Buffer Capacity

$s(t)$: Energy state

Where:

$$H(t) = \int_0^t P_H(\tau) d\tau + s(0) \quad C(t) = \int_0^t P_C(\tau) d\tau$$

Shaded area = $s(t)$

Packet Transmission

Packet Lost due to Energy Outage

Where:

$$e_H^k = e_H^k - e_C^k + s^k$$

Subject to: $0 \leq s^{k+1} \leq C_B$

$$e_H^k = \int_{t_k}^{t_{k+1}} P_H(t) dt$$

e_C^k = Provided by the application

"Scalability of Network Capacity in Energy-Harvesting-Enabled Wireless Sensor Networks", Raul Gomez Cid-Fuentes, Albert Cabellos, Eduard Alarcon, IEEE Transactions on Networking, 2014.

Using the Ambient Energy model: temporal storage dimensioning and network capacity scalability

N3Cat

- Scalability
 - Define Energy Path Function:
$$U_C = \frac{E_C}{C_B} = h\left(\frac{E_H}{C_B}\right) = h(U_H)$$
 - It is found that the network scales as: $\tilde{\Theta}(h(n^{-\alpha/2})n^{\alpha-1/2})$
 - RF Example:
 - Spatio-Temporal Correlation
- Energy Buffer Dimensioning
 - The energy buffer must store energy to overcome slow fadings in the energy harvesting.
 - RF Example with Rayleigh Channel:
 - Harvested Power [dBm] vs Time [min]. The plot shows a highly fluctuating signal with several deep fades.
 - Stored Energy [μJ] vs Time [min]. The plot shows the energy buffer level over time, with red circles highlighting periods of low energy levels labeled as 'Energy Outage'.
 - Time-varying evaluation of the Energy Outage (no steady state):
 - Energy Outage Probability vs Energy Buffer Size, C_B [mJ]. The plot shows the probability of an outage occurring within a certain time interval t_o for different values of t_o (10, 100, 1000 s).
 - Average Time to Energy Outage [hours] vs Energy Buffer Capacity [mJ]. The plot shows the average time until an outage occurs as a function of the energy buffer capacity.

Wireless power transfer: Team and projects

N3Cat

- Project: Resonant Inductive Near-field Generation System (RINGS)
 - Sponsors:** Defense Advanced Research Projects Agency (DARPA), National Aeronautics and Space Administration (NASA)
 - Collaborators:** David Miller (Co-I), Peter Fisher, Alex Buck, Greg Eslinger (MIT), John Merk (Co-I), Roedolph Opperman (Aurora Flight Sciences), Elisenda Bou (UPC Barcelona Tech)
- Project proposals:** Google Inc

Elisenda Bou, PhD candidate

UNIVERSITAT POLITÈCNICA
DE CATALUNYA
BARCELONATECH

Dr. Ray Sedwick

UNIVERSITY OF MARYLAND

Prof. Eduard Alarcón (EE)

UNIVERSITAT POLITÈCNICA
DE CATALUNYA
BARCELONATECH

Prof. Peter Fisher
(MIT Dept Physics)

Massachusetts Institute of Technology

Energy Harvesting concept extension: active energy mothership

UPC work on Resonant inductive coupling WPT

Open challenges in Resonant inductive coupling wireless power transfer:

- Distance-insensitive WPT power link: adaptive high-efficiency impedance matching

• Overall system efficiency

• IIMO 9WPT system

• Class E2 Resonant Non-Radiative Wireless Power Transfer Link: A design-oriented joint circuit-system co-characterization approach”, Elisenda Bou-Balust, Tomoharu Nagashima, Hiroto Sekiyama, Eduard Alarcon

• Scalability Analysis of SIMO Non-Radiative Resonant Wireless Power Transfer Systems based on Circuit Models”, Elisenda Bou-Balust, Raymond Sedwick and Eduard Alarcon

$$\begin{pmatrix} I_1 \\ I_2 \\ \vdots \\ I_n \end{pmatrix} = \begin{pmatrix} 0 & G_{21}G_1 & \dots & G_{n1}G_1 \\ G_{12}G_2 & 0 & \dots & G_{n2}G_2 \\ \vdots & \ddots & \ddots & \vdots \\ G_{1n}G_n & G_{2n}G_n & \dots & 0 \end{pmatrix} \begin{pmatrix} I_1 \\ I_2 \\ \vdots \\ I_n \end{pmatrix} + \begin{pmatrix} V_{in,1}G_1 \\ V_{in,2}G_2 \\ \vdots \\ V_{in,n}G_n \end{pmatrix}$$

$$\eta_{N,RP} = \frac{|I_1|^2 R_{L,1}}{\sum_{i=0}^{N-1} |I_i|^2 R(Z_i) + \sum_{i=0}^{N-1} |I_i|^2 R(Z_i)}$$

Fig. 1: Multi-Node RIC WPT System

$$\eta_{RP} = \frac{G_p G_t G_{tp}}{4 G_p^2 G_{tp}^2 - G_p (4 G_{tp} - (N-1) G_{tr}^2 G_t) + 1}$$

Chaotic nonlinear dynamics in RIC-WPT

N3Cat

Chaotic oscillation of RIC-WPT with nonlinear saturable inductors

$$\begin{aligned} \mathbf{x}(t) &= e^{\mathbf{A}_i(t-t_i)} \mathbf{x}(t_i) + \int_{t_i}^t e^{\mathbf{A}_i(t-\tau)} \mathbf{B}_i(\tau) d\tau \\ &:= \Phi_i(t-t_i) \mathbf{x}(t_i) + \Psi_i(t, t_i) \end{aligned}$$

$$\Psi_i(t, t_i) = (\Lambda_i^2 + \omega_f^2)^{-1} [\Phi_i(t-t_i)(\omega_f \cos(\omega_f t) \\ + A_i \sin(\omega_f t)) - \omega_f I \cos(\omega_f t) \\ - A_i \sin(\omega_f t)] \mathbf{B}$$

$$\dot{\mathbf{x}} = \mathbf{A}_i \mathbf{x} + \mathbf{B}_i := \mathbf{f}_i(\mathbf{x})$$

$$\mathbf{A}_i = \begin{pmatrix} \frac{L_p i_p}{\Delta(i_p)} & \frac{M}{\Delta(i_p)} & \frac{L_s}{\Delta(i_p)} \\ \frac{M}{\Delta(i_p)} & \frac{L_p i_p R}{\Delta(i_p)} & \frac{M}{\Delta(i_p)} \\ \frac{1}{C_p} & 0 & 0 \\ 0 & \frac{1}{C_s} & 0 \end{pmatrix}$$

$$\mathbf{B}_i = \begin{pmatrix} \frac{V_{in} L_p}{\Delta(i_p)} \sin(\omega_f t) \\ \frac{V_{in} M}{\Delta(i_p)} \sin(\omega_f t) \\ 0 \\ 0 \end{pmatrix}, \mathbf{x} = \begin{pmatrix} i_p \\ i_s \\ v_p \\ v_s \end{pmatrix}$$

Unveiling Nonlinear Dynamics in a Resonant Inductively Coupled Wireless Power Transfer Circuit, E. Bou-Balust, A. el Aroudi, P. Fisher, E. Alarcon, IEEE ISCAS 2014 Melbourne, special session (UPC / MIT / URV)

UNIVERSITAT POLITÈCNICA DE CATALUNYA BARCELONATECH

Embedding energy processing frontends in RIC-WPT

N3Cat

Resonant Inductive Coupled Wireless Power Transfer With Class-E2 DC-DC Converter for high efficiency

(a)

(b)

(c)

(d)

(e)

(f)

Class-E inverter Transformer Class-E rectifier

(b)

(c)

$v_S(2\pi) = 0 \quad \text{and} \quad \left. \frac{dv_S}{dt} \right|_{t=2\pi} = 0.$

Power delivery efficiency η (%)

Design value

$$\eta_{max} = \frac{k^2 \omega^2 L_1 L_2 R_0}{R_0 (R_0 + R_{L2})^2 + k^2 \omega^2 L_1 L_2 (R_0 + R_{L2})},$$

$$C_S = \frac{2 \sin(\pi D_S) \cos(\pi D_S + \phi_S) \sin(\pi D_S + \phi_S) [(1 - D_S) \pi \cos(\pi D_S) + \sin(\pi D_S)]}{\omega \pi^2 (1 - D_S) R_1}.$$

UNIVERSITAT POLITÈCNICA DE CATALUNYA BARCELONATECH

Interference analysis in RIC-WPT

N3Cat

Model predicting effect of interfering objects on frequency detuning

Power Transfer Efficiency

$$\eta = \frac{(\omega M_{12})^2 Z_L Z_t}{Z_1(Z_2 + R_L)^2 Z_t + (\omega M_{12})^2 (Z_2 + R_L) Z_t + (\omega M_{11})^2}$$

Backplane metallic object.
RING testbed for WPT/FF
oriented to ISS

© "Interference analysis on Resonant Inductive Coupled Wireless Power Transfer Links", Elisenda Bou-Balust, Eduard Alarcon , Raymond Sedwick and Peter Fisher, IEEE ISCAS 2013 Beijing, (UPC/Maryland/MIT)

UNIVERSITAT POLITÈCNICA
DE CATALUNYA
BARCELONATECH

UPC work on Resonant inductive coupling WPT

N3Cat

On-going applications:

- Fractionated spacecrafts / nanosatellite constellation / flight formation

2013-4-26 11:31:13AM

UNIVERSITAT POLITÈCNICA
DE CATALUNYA
BARCELONATECH

